LETTER
SPACE PHYSICS: GEOELECTROMAGNETICS

Earth and Planetary Physics
8: 565–569, 2024
doi: 10.26464/epp2024047

Recent geomagnetic storms observed by Macau Science Satellite-1

Qing Yan, and HongBo Yao*

Macau Institute of Space Technology and Application, Macau University of Science and Technology, Macao 999078, China

Key Points:

- Initial magnetic data measured by Macau Science Satellite-1 (MSS-1) were processed and analyzed.
- Magnetic signals related to geomagnetic storms during March 24–25, 2024 and May 10–12, 2024 were detected clearly by MSS-1.
- Geoelectric fields induced in the Earth rapidly increased during these geomagnetic storms.

Citation: Yan, Q., and Yao, H. B. (2024). Recent geomagnetic storms observed by Macau Science Satellite-1. *Earth Planet. Phys.*, *8*(4), 565–569. http://doi.org/10.26464/epp2024047

Abstract: Geomagnetic storms are rapid disturbances of the Earth's magnetosphere. They are related to many geophysical phenomena and have large influences on human activities. Observing and studying geomagnetic storms is thus of great significance to both scientific research and geomagnetic hazards prevention. The Macau Science Satellite-1 (MSS-1) project includes two high-precision Chinese geomagnetic satellites successfully launched on May 21, 2023. The main purpose of MSS-1 is to accurately measure the Earth's magnetic field. Here, we analyze early MSS-1 geomagnetic field measurements and report observations of two recent geomagnetic storms that occurred on March 24, 2024 and May 11, 2024. We also calculate the related geoelectric fields as an initial step towards a quantitative assessment of geomagnetic hazards.

Keywords: Macau Science Satellite-1; geomagnetic storms; satellite magnetics; electromagnetic induction; geoelectric fields

1. Introduction

Geomagnetic storms are rapid disturbances of the Earth's magnetosphere caused by enhanced interaction between the solar wind and Earth's magnetosphere (Gonzalez et al., 1994). Many geophysical phenomena are associated with or caused by geomagnetic storms, such as geomagnetically induced currents (Pulkkinen et al., 2017) and ionospheric disturbances (Mendillo, 2006). Super geomagnetic disturbances can lead to disruption of electrical systems, satellite hardware damage, communication failures, and navigation problems (Lakhina and Tsurutani, 2016).

The MSS-1 is the world's first low-inclination (about 41°) geomagnetic satellite mission. It is composed of two satellites, MSS-1A and MSS-1B, successfully launched on May 21, 2023 into near-circular orbits of 450 km altitude (Zhang K, 2023). MSS-1A is equipped with a highly stable optical bench, a high-precision fluxgate magnetometer, and a high-precision scalar magnetometer; it can measure the Earth's magnetic field with unprecedented accuracy. MSS-1B is equipped with an energetic electron spectrometer and a solar X-ray detector; its main objective is to monitor solar activities and their effects on the Earth's space plasma.

During geomagnetic storms, the strength of the ring current in the magnetosphere increases significantly, generating large and rapid geomagnetic disturbances. Therefore, high-precision geomagnetic observations such as those of the MSS-1 satellites have significant potential to improve understanding of geomagnetic storms and to provide warnings early enough to avoid serious storm damage. In this work, we analyze early MSS-1 geomagnetic field measurements, focusing especially on data collected during two recent geomagnetic storms, which occurred during March 24–25, 2024 and May 10–12, 2024. We also use two realistic radial Earth's conductivity models to calculate model-predicted geoelectric fields induced by the observed geomagnetic storms.

First author: Yan Q., qingyan2317@gmail.com
Correspondence to: Yao H. B., hongbo.yao@outlook.com
Received 04 JUN 2024; Accepted 25 JUN 2024.
First Published online 01 JUL 2024.

2. Data and Method

2.1 Data Collection and Preprocessing

We collected MSS-1 vector magnetic field data from March and May, 2024, during which intense solar activities were reported. The original vector magnetic measurements have been calibrated and rotated from the instrument frame to the north-east-center frame (Yan Q et al., 2023). The root-mean-squared difference between scalar and vector magnetic measurements is below 0.5 nT, indicating the good quality of the data. Figure 1 shows the global distribution of MSS-1 vector data points on May 11, 2024. Due to the unique low-inclination MSS-1 orbit, the measurements are distributed at middle and low latitudes. This configuration can provide an excellent local time sampling of the Earth's magnetic field.

2.2 Extraction of Geomagnetic Storm-Related Magnetic Signals

The observed magnetic field includes mainly the contributions

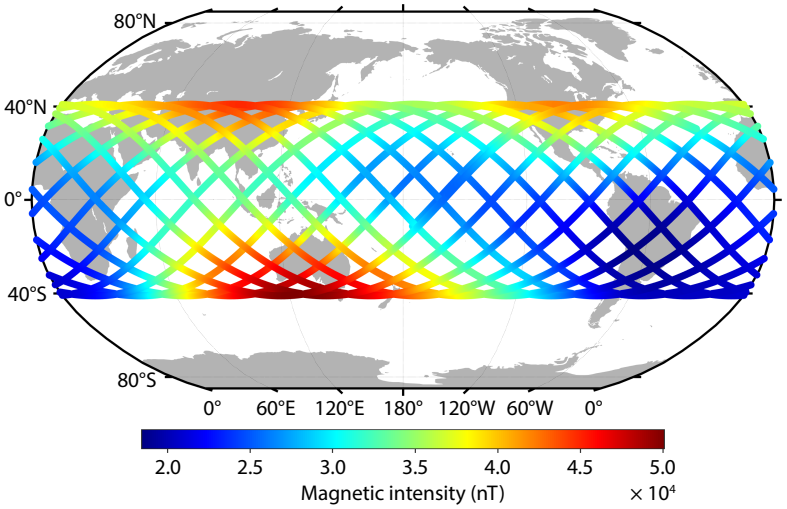

Figure 1. Illustration of the global distribution of MSS-1 vector magnetic data on May 11, 2024 with colorbar indicating the corresponding magnetic intensity.

from the Earth's core and crust, the magnetospheric and ionospheric current systems, and their Earth-induced counterparts (Finlay et al., 2020; Sabaka et al., 2020). To describe the disturbed magnetic field due to geomagnetic storms, we use the following magnetic residual

$$\Delta \boldsymbol{B} = \boldsymbol{B}_{\rm obs} - \boldsymbol{B}_{\rm mod}, \tag{1}$$

where $\boldsymbol{B}_{\rm obs}$ denotes the observed magnetic field and $\boldsymbol{B}_{\rm mod}$ denotes the core and crustal fields as predicted by the CHAOS-7 geomagnetic field model (Finlay et al., 2020). After removing the day-time magnetic field, the residual magnetic field $\Delta\boldsymbol{B}$ is mainly due to the large-scale magnetospheric ring current and can be represented by the negative gradient of a magnetic scalar potential V, that is $\Delta\boldsymbol{B} = -\nabla V$. The magnetic scalar potential is approximated by spherical harmonic expansion in the geomagnetic coordinate system (Laundal and Richmond, 2017):

$$V(r, \theta_{\rm gm}, \phi_{\rm gm}, t) = a\left[e_1^0(t)\left(\frac{r}{a}\right) + i_1^0(t)\left(\frac{a}{r}\right)^2\right]P_1^0(\cos\theta_{\rm gm}), \tag{2}$$

where r, $\theta_{\rm gm}$, $\phi_{\rm gm}$ are the radial distance from Earth's center, the geomagnetic colatitude, and the geomagnetic longitude, respectively; t denotes the time dependence of the magnetic field; a is the Earth's mean radius; $P_1^0(\cos\theta_{\rm gm}) = \cos\theta_{\rm gm}$ is the Schmidt quasi-normalized associated Legendre function of degree 1 and order 0; e_1^0 is the external coefficient describing the strength of the magnetospheric ring current; and i_1^0 is the corresponding induced coefficient due to electromagnetic induction in the Earth's interior. The magnetic field components can be written as

$$\begin{aligned} B_r(r, \theta_{\rm gm}, \phi_{\rm gm}, t) &= \left[-e_1^0(t) + 2i_1^0(t)\left(\frac{a}{r}\right)^3\right]\cos\theta_{\rm gm}, \\ B_\theta(r, \theta_{\rm gm}, \phi_{\rm gm}, t) &= \left[e_1^0(t) + i_1^0(t)\left(\frac{a}{r}\right)^3\right]\sin\theta_{\rm gm}, \\ B_\phi(r, \theta_{\rm gm}, \phi_{\rm gm}, t) &= 0, \end{aligned} \tag{3}$$

where B_r, B_θ, B_ϕ are the radial, colatitude, and longitude components in the geomagnetic coordinate system. Using the residual field to fit above equations, we can estimate the time series of the external and induced coefficients (Yao HB et al., 2023). The external coefficients represent the magnetic signals related to geomagnetic storms.

3. Results

3.1 Geomagnetic Storms during March 24–25, 2024 and May 10–12, 2024

Figure 2a illustrates the time series of magnetospheric external (blue color) and induced coefficients (red color) recovered from MSS-1 vector magnetic data of March 2024. Compared to the external coefficients, the induced coefficients have a smaller amplitude but show the same characteristics. Therefore, we concentrate on the external coefficients in the following parts. Multiple spikes on and around March 24 are observed, which reflect temporary disturbances of the Earth's magnetosphere. The maximum external coefficient is greater than 100 nT during 16:00–18:00 Coordinated Universal Time (UTC). The Disturbance Storm-Time (*Dst*) index (https://wdc.kugi.kyoto-u.ac.jp/dstdir/), which is derived from geomagnetic observatory data and is traditionally used for monitoring geomagnetic disturbances, is also less than −100 nT during 16:00–18:00 UTC. Therefore, the observed maximum spike is associated with the strong geomagnetic storm (Loewe and Prölss, 1997) that occurred on March 24, 2024.

Similarly, Figure 2b shows the time series of magnetospheric external and induced coefficients in May 2024. Compared to the spike of March 2024, the spike at around 03:00 UTC, May 11, is more clearly visible. The time series on and around May 11 show more distinctly the characteristics of a geomagnetic storm. At 12:00 UTC, May 10, the external coefficients decrease slowly, indicating the initial phase of a geomagnetic storm. Then, the external coefficients increase rapidly and reach maximum values that are close to 400 nT. This is a typical characteristic during the main phase of a geomagnetic storm. Finally, the external coefficients decrease gradually, indicating the recovery phase of a geomagnetic storm. These observed characteristics are consistent with those of the *Dst* index. At 03:00 UTC, May 11, the *Dst* index peaks at −412 nT. The above results demonstrate that MSS-1 have

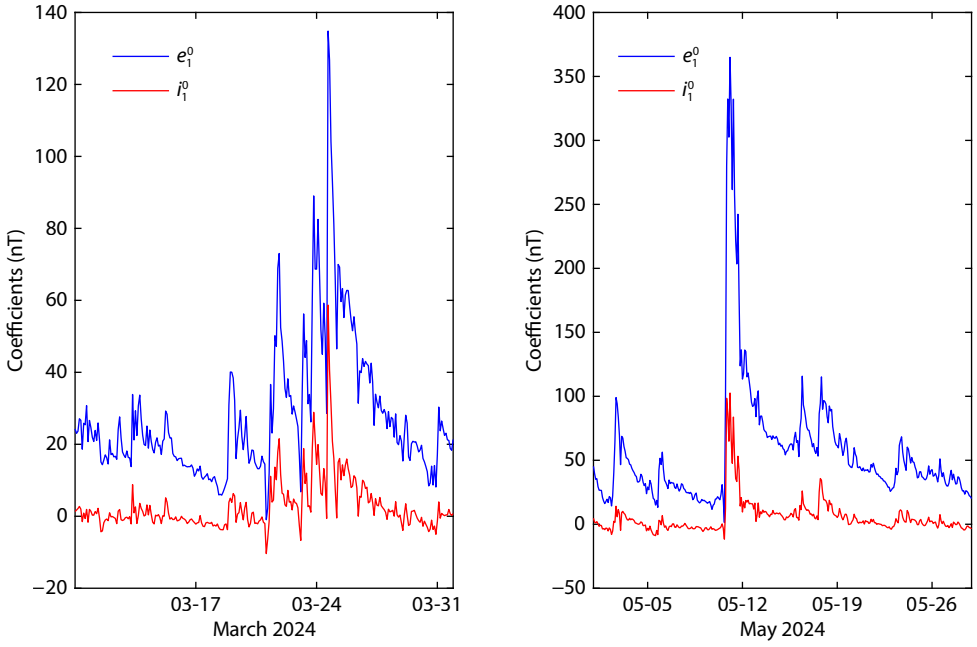

Figure 2. Time series of magnetospheric external (e_1^0) and induced (i_1^0) coefficients for March 2024 (left) and May 2024 (right). Spikes that occurred during March 24–25, 2024 and May 10–12, 2024 are magnetic signals related to geomagnetic storms.

clearly observed that a great geomagnetic storm (Loewe and Prölss, 1997) occurred on May 11, 2024.

3.2 The Geoelectric Fields Induced in the Earth

According to Faraday's laws of electromagnetic induction, time-varying magnetic fields will generate electric fields and induce currents in the conductive Earth and in electrical power systems (Pulkkinen et al., 2017). As shown in Figure 2b, the strength of the external source coefficients rapidly increased by a factor of more than 10 during the geomagnetic storm that occurred on May 11, 2024 (from ~25 nT to ~350 nT). Therefore, the induction of large electric fields and currents in electrical power systems in that very short time was to be expected. In the absence of precautions, such geomagnetically induced currents could lead to severe damage in electric power grids and pipelines.

Here, we estimate the geoelectric fields due to the geomagnetic storm that occurred on May 11, 2024 by solving Maxwell's electromagnetic induction equations. For simplicity, globally averaged one-dimensional (1D) Earth's conductivity models are used to account for the induction. Here, we consider two different global 1D conductivity models (Civet et al., 2015; Yao HB et al., 2023) that are designed to show the influences of conductivity on the induced geoelectric fields (Figure 3). To simulate the time series of the geoelectric fields, we implemented a simple time domain method, which consists of three steps: (i) transform the time series of the external source coefficients e_1^0 into the frequency domain by Fourier transform; (ii) calculate the frequency domain electric fields with a recursive formulation (Kuvshinov and Semenov, 2012) as implemented in a previous forward modeling solver (Yao HB et al., 2022); (iii) transform the frequency domain electric fields into the time domain by inverse Fourier transform.

Figure 4 shows the time series of the E_ϕ component of geoelectric fields in different regions of the world in May, 2024. It can be observed that the influence of geomagnetic storms is global. During geomagnetic storms, the geoelectric fields show distinct oscillation characteristics. The amplitude of geoelectric fields in May, 2024, increased rapidly by a factor of more than 10 compared to that of quiet times, further demonstrating the potential severe hazards of great geomagnetic storms. The calculation of geoelectric fields provides an initial step towards a quantitative assessment of geomagnetic hazards. We should note that the result shown in Figure 4 is a rough estimation of the induced geoelectric fields. Higher accuracy in the modeling of geoelectric fields due to geomagnetic storms can be achieved in the future by considering a more realistic magnetospheric current source. Besides, we can also observe that the amplitudes of the simulated geoelectric fields are influenced by conductivity structures. There-

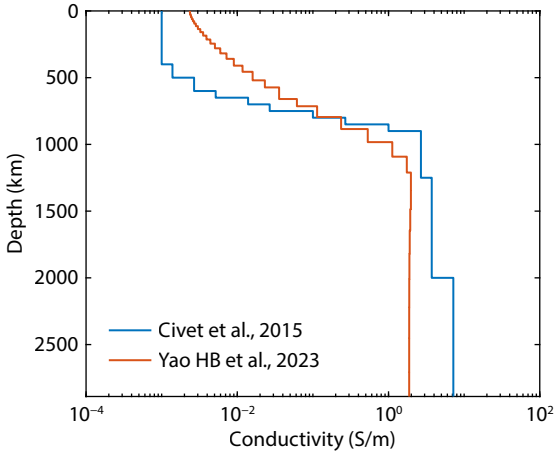

Figure 3. Global averaged Earth's conductivity models (Civet et al., 2015; Yao HB et al., 2023) used to compute the geoelectric fields due to geomagnetic storms.

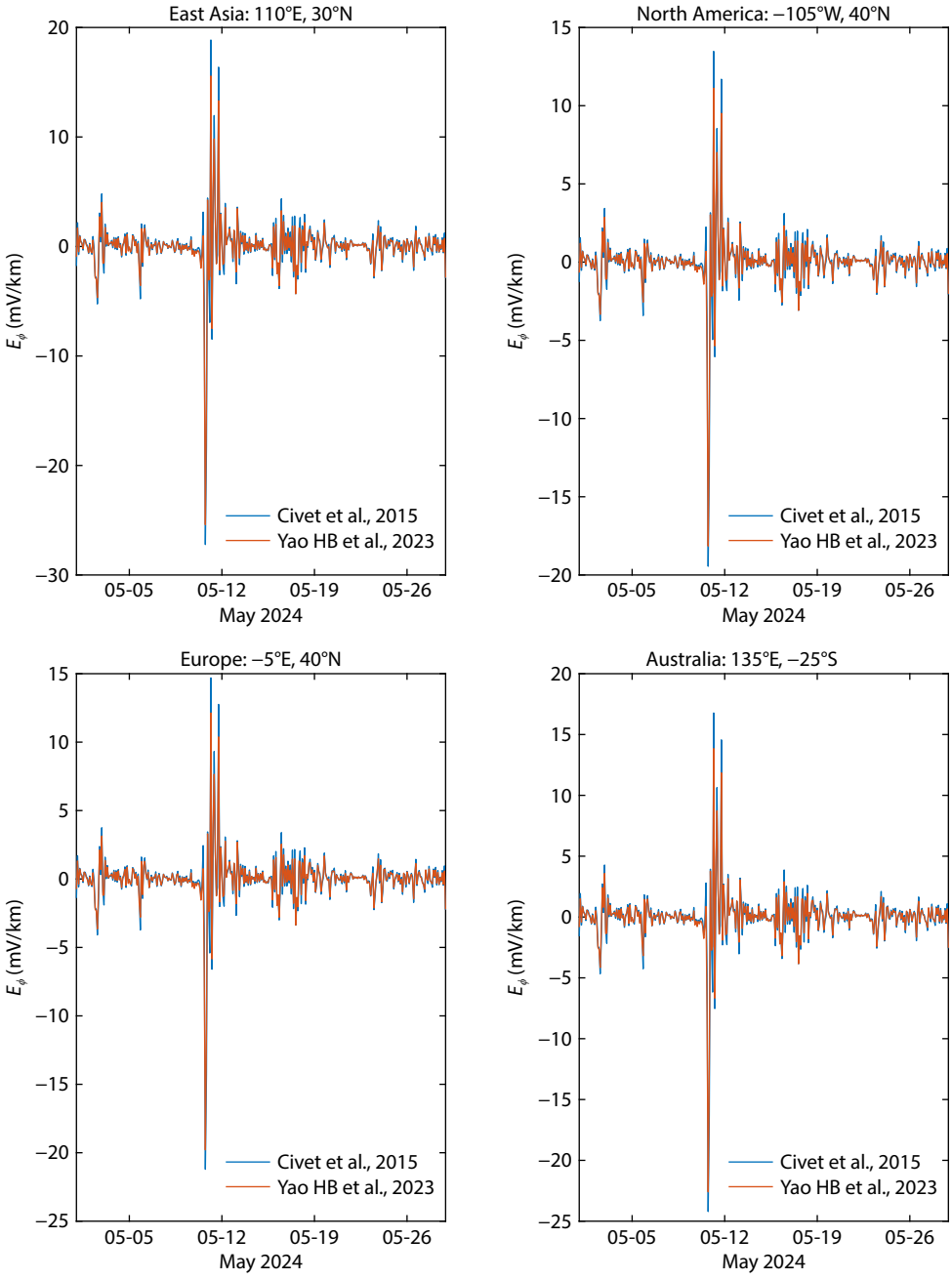

Figure 4. Time series of Earth's surface E_ϕ component of geoelectric fields in different regions, as simulated using the two different conductivity models (see Figure 3).

fore, considering a more realistic three-dimensional (3D) Earth's conductivity structure (Püthe and Kuvshinov, 2013) will also improve the accuracy of modeling.

4. Conclusions

We have processed and analyzed early magnetic field measurements from the recently-operational MSS-1 mission. After correcting for the Earth's core and crustal fields and removing day-time data, magnetic signals attributable to the large-scale magnetospheric ring current were extracted. The extracted magnetic signals show that MSS-1 clearly detected a strong geomagnetic storm on March 24, 2024 and a great geomagnetic storm on May 11, 2024. We calculated the geoelectric fields due to the geomagnetic storm that occurred on May 11, 2024 by considering two realistic radial Earth's conductivity models. Our calculations show that the geoelectric fields induced in the Earth increased rapidly during the May 11, 2024 geomagnetic storm. Based on the above results, MSS-1 observations may be able to play an important role in assessing geomagnetic storms and preventing the disruptions and damage that some storms could cause to important social infrastructure.

We should note that the results reported here are preliminary. Future work should focus on the following aspects. First, data quality may be further improved by optimizing data processing procedures. Second, accuracy of the calculation of geoelectric

fields due to geomagnetic disturbances can be improved by considering a more realistic magnetospheric current source and by using a more realistic 3D Earth's conductivity model. Finally, quantitative estimation of geomagnetic induced currents and assessment of geomagnetic hazards can be achieved by incorporating power grid system models.

Acknowledgments

This work was supported financially by the National Natural Science Foundation of China (42250101), and the Macau Foundation and Macau Science and Technology Development Fund (0001/2019/A1). We would like to thank Professor Keke Zhang for insightful discussions and MSS-1 team members for supporting and managing the satellite project. We thank the Editor and two anonymous reviewers for their helpful suggestions and comments. We also thank EPP's guest copyeditor Mr. David Eisenman for improving the English presentation of this paper.

References

Civet, F., Thébault, E., Verhoeven, O., Langlais, B., and Saturnino, D. (2015). Electrical conductivity of the Earth's mantle from the first Swarm magnetic field measurements. *Geophy. Res. Lett.*, *42*(9), 3338–3346. https://doi.org/10.1002/2015GL063397

Finlay, C. C., Kloss, C., Olsen, N., Hammer, M. D., Tøffner-Clausen, L., Grayver, A., and Kuvshinov, A. (2020). The CHAOS-7 geomagnetic field model and observed changes in the South Atlantic Anomaly. *Earth, Planets Space, 72*(1), 156. https://doi.org/10.1186/s40623-020-01252-9

Gonzalez, W. D., Joselyn, J. A., Kamide, Y., Kroehl, H. W., Rostoker, G., Tsurutani, B. T., and Vasyliunas, V. M. (1994). What is a geomagnetic storm?. *J. Geophys. Res.: Space Phys.*, *99*(A4), 5771–5792. https://doi.org/10.1029/93JA02867

Kuvshinov, A., and Semenov, A. (2012). Global 3-D imaging of mantle electrical conductivity based on inversion of observatory *C*-responses-I. An approach and its verification. *Geophys. J. Int.*, *189*(3), 1335–1352. https://doi.org/10.1111/j.1365-246X.2011.05349.x

Lakhina, G. S., and Tsurutani, B. T. (2016). Geomagnetic storms: historical perspective to modern view. *Geosci. Lett.*, *3*(1), 5. https://doi.org/10.1186/s40562-016-0037-4

Laundal, K. M., and Richmond, A. D. (2017). Magnetic coordinate systems. *Space Sci. Rev.*, *206*(1-4), 27–59. https://doi.org/10.1007/s11214-016-0275-y

Loewe, C. A., and Prölss, G. W. (1997). Classification and mean behavior of magnetic storms. *J. Geophys. Res.: Space Phys.*, *102*(A7), 14209–14213. https://doi.org/10.1029/96JA04020

Mendillo, M. (2006). Storms in the ionosphere: patterns and processes for total electron content. *Rev. Geophys.*, *44*(4), RG4001. https://doi.org/10.1029/2005RG000193

Pulkkinen, A., Bernabeu, E., Thomson, A., Viljanen, A., Pirjola, R., Boteler, D., Eichner, J., Cilliers, P. J., Welling, D., … MacAlester, M. (2017). Geomagnetically induced currents: Science, engineering, and applications readiness. *Space Weather*, *15*(7), 828–856. https://doi.org/10.1002/2016SW001501

Püthe, C., and Kuvshinov, A. (2013). Towards quantitative assessment of the hazard from space weather. global 3-D modellings of the electric field induced by a realistic geomagnetic storm. *Earth, Planets Space, 65*(9), 1017–1025. https://doi.org/10.5047/eps.2013.03.003

Sabaka, T. J., Tøffner-Clausen, L., Olsen, N., and Finlay, C. C. (2020). CM6: A comprehensive geomagnetic field model derived from both CHAMP and Swarm satellite observations. *Earth, Planets Space, 72*(1), 80. https://doi.org/10.1186/s40623-020-01210-5

Yan, Q., Ou, J. M., Suo, L., Jiang, Y., and Liu, P. F. (2023). Study on the estimation of Euler angles for Macau Science Satellite-1. *Earth Planet. Phys.*, *7*(1), 144–150. https://doi.org/10.26464/epp2023017

Yao, H. B., Ren, Z. Y., Tang, J. T., and Zhang, K. K. (2022). A multi-resolution finite-element approach for global electromagnetic induction modeling with application to Southeast China coastal geomagnetic observatory studies. *J. Geophys. Res.: Solid Earth*, *127*(8), e2022JB024659. https://doi.org/10.1029/2022JB024659

Yao, H. B., Ren, Z. Y., Pan, K. J., Tang, J. T., and Zhang, K. K. (2023). A global mantle conductivity model derived from 8 years of Swarm satellite magnetic data. *Earth Planet. Phys.*, *7*(1), 49–56. https://doi.org/10.26464/epp2023011

Zhang, K. K. (2023). A novel geomagnetic satellite constellation: science and applications. *Earth Planet. Phys.*, *7*(1), 4–21. https://doi.org/10.26464/epp2023019